Supporting Information

Rec. Nat. Prod. **16:3 (2022) 212-224**

Anti-Obesity and Antihyperlipidemic Effects of *Musa cavendishii*

Mohammed S. Abdel-Raziq[1,2], Fatma M. Abdel Bar[3,4], Sylvia A. Ashamallah[5], Nashwa Barakat[6] and Ahmed A. Gohar[1]

[1] *Department of Pharmacognosy, Faculty of Pharmacy, Mansoura University, Mansoura 35516, Egypt*

[2] *School of Chemistry and Molecular Biosciences, University of Queensland, St Lucia 4072, Queensland, Australia*

[3] *Department of Pharmacognosy, Faculty of Pharmacy, Prince Sattam Bin Abdulaziz University, Al-Kharj 11942, Saudi Arabia*

[4] *Faculty of Pharmacy, Mansoura University, Mansoura 35516, Egypt*

[5] *Pathology Department, Faculty of Medicine, Mansoura University, Mansoura 35516, Egypt*

[6] *Animal Research Facility, Urology and Nephrology Center, Mansoura University, Mansoura 35516, Egypt*

Table of content **Page**

Figure S1:	Histological analysis of C57BL/6J mice groups' liver stained with Hematoxylin and Eosin stain (X100). Treated groups are (a) High fat diet, HFD; (b) Low fat diet, LFD; (c) Green tea total extract, HFD+GTE; (d) *M. cavendishii* total leaf extract, HFD+TLE; (e) *n*-Hexane fraction, HFD+Hex; (f) EA fraction, HFD+EA.	3
Figure S2:	Histological analysis of liver from High Fat Diet (HFD).	4
Figure S3:	Histological analysis of liver from control group with normal diet.	5
Figure S4:	Histological analysis of liver from treated with green tea total extract group with HFD.	6
Figure S5:	Histological analysis of liver from group treated with *M. cavendishii* total extract.	7
Figure S6:	Histological analysis of liver from group treated with the ethyl acetate fraction of *M. cavendishii*.	8

© 2021 ACG Publications. All rights reserved.

Figure S7:	Histological analysis of liver from group treated with "*n*-hexane fraction of *M. cavendishii*.	9
Figure S8:	Representative CT images segmented for fat (axial, coronal and sagittal slices). A: *M. cavendishii* group CT, fat volume in blue, B: HFD CT, fat volume in blue, and C: LFD CT group, fat volume in blue.	10
Figure S9:	Representative CT images segmented for fat (axial, coronal and sagittal slices). A: *n*-hexane fraction of *M. cavendishii* group CT, fat volume in blue, B: HFD CT, fat volume in blue and C: LFD CT group, fat volume in blue.	11
Figure S10:	Representative CT images segmented for fat (axial, coronal and sagittal slices). A: Ethyl acetate fraction of *M. cavendishii* group CT, fat volume in blue, B: HFD CT, fat volume in blue and C: LFD CT group, fat volume in blue.	12
Figure S11:	Representative CT images segmented for fat (axial, coronal and sagittal slices). A: Green tea total extract group CT, fat volume in blue, B: HFD CT, fat volume in blue, and C: LFD CT group, fat volume in blue.	13
	Phytochemical investigation of the *n*-hexane fraction of *Musa cavendeshii*.	14
Table S1:	^{1}H NMR (500 MHz) and APT (125 MHz) spectral data of compound **2** in chloroform-*d*	15
Figure S12:	^{1}H NMR (500 MHz) spectrum of compound **2** in $CDCl_3$.	16
Figure S13:	APT (125 MHz) spectrum of compound **2** in $CDCl_3$.	17
Figure S14:	HSQC spectrum of compound **2**.	18
Figure S15:	HMBC spectrum of compound **2** in $CDCl_3$.	19
Figure S16:	HRMS spectrum of compound **2**.	20
Table S2.:	^{1}H NMR (500 MHz) and APT (125 MHz) spectral data of compound **3** in chloroform-*d*.	21
Figure S17:	^{1}H NMR (500 MHz) spectrum of compound **3** in $CDCl_3$.	22
Figure S18:	APT (125 MHz) spectrum of compound 3 in $CDCl_3$.	23

© 2021 ACG Publications. All rights reserved.

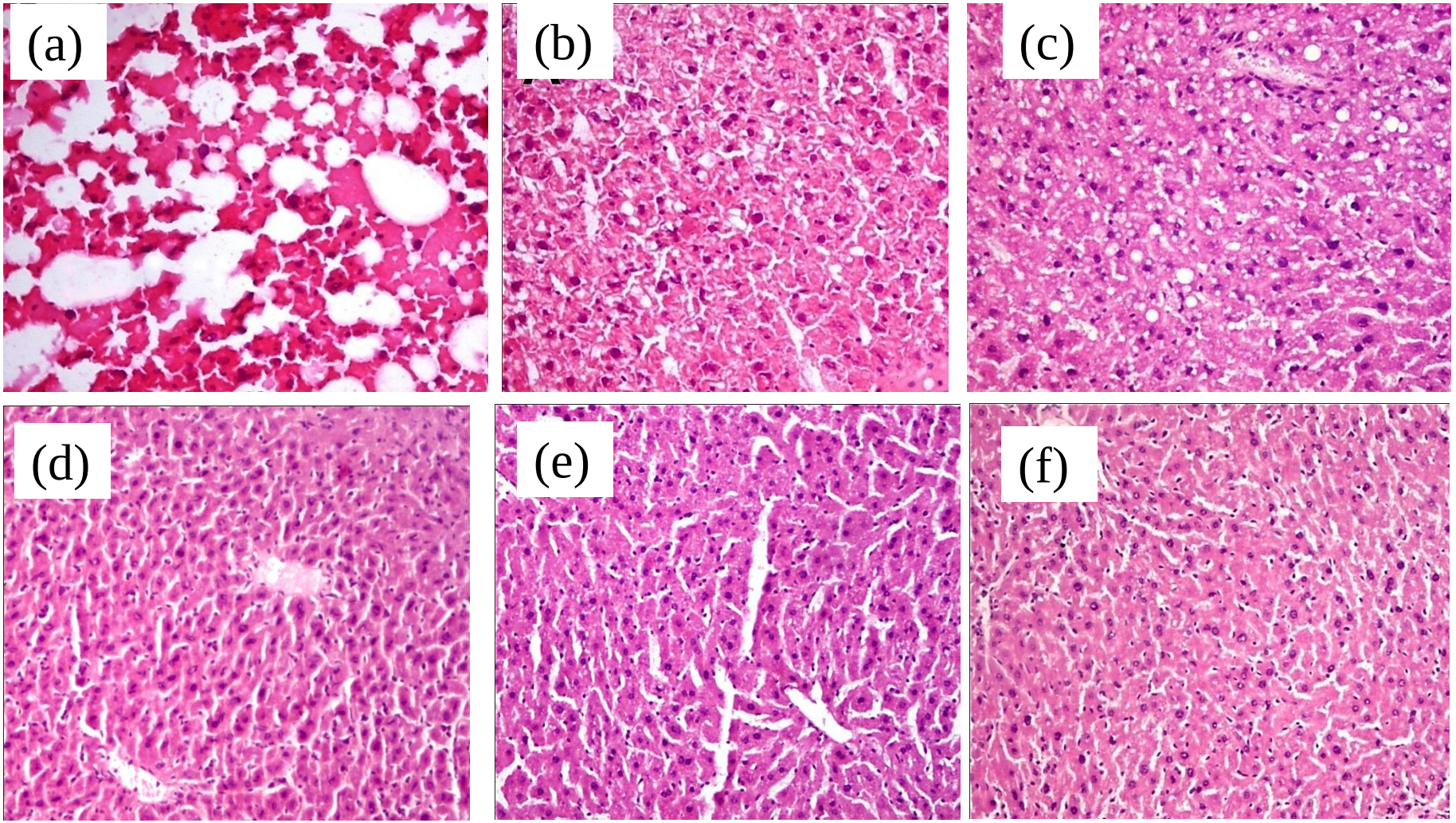

Figure S1: Histological analysis of C57BL/6J mice groups' liver stained with Hematoxylin and Eosin stain (X100). Treated groups are (a) High fat diet, HFD; (b) Low fat diet, LFD; (c) Green tea total extract, HFD+GTE; (d) *M. cavendishii* total leaf extract, HFD+TLE; (e) *n*-Hexane fraction, HFD+Hex; (f) EA fraction, HFD+EA.

© 2021 ACG Publications. All rights reserved.

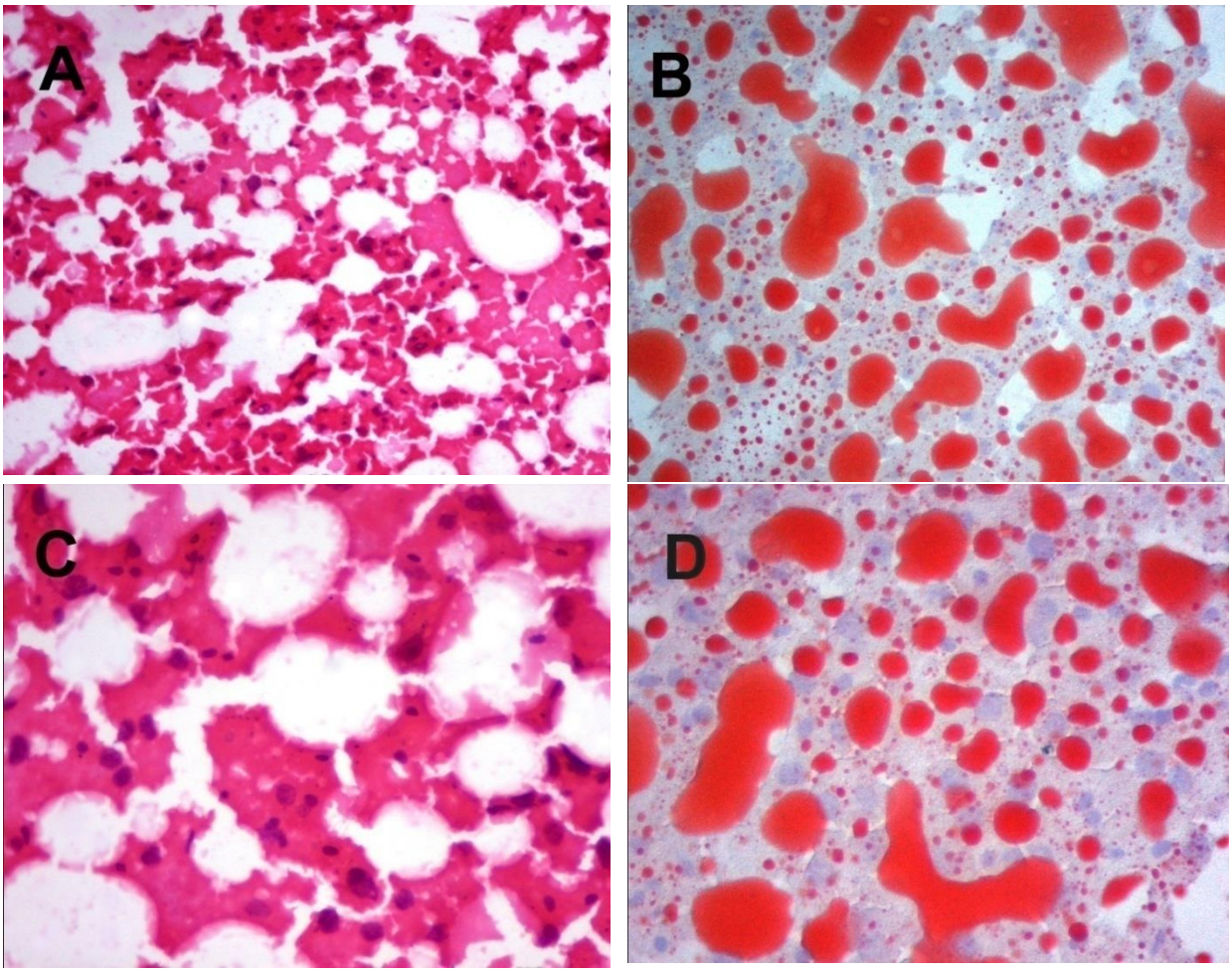

Figure S2: Histological analysis of liver from High Fat Diet (HFD). A: Hematoxylin and Eosin stain (X100) reveals near normal liver architecture with marked mainly macrovesicular steatosis in hepatocytes seen as clear unstained spaces. B: Oil Red O stain (X100), performed on frozen liver sections. Numerous large lipid droplets are seen within hepatocytes as red-stained dots. C&D: higher magnification of the previous two photomicrographs respectively (X200).

© 2021 ACG Publications. All rights reserved.

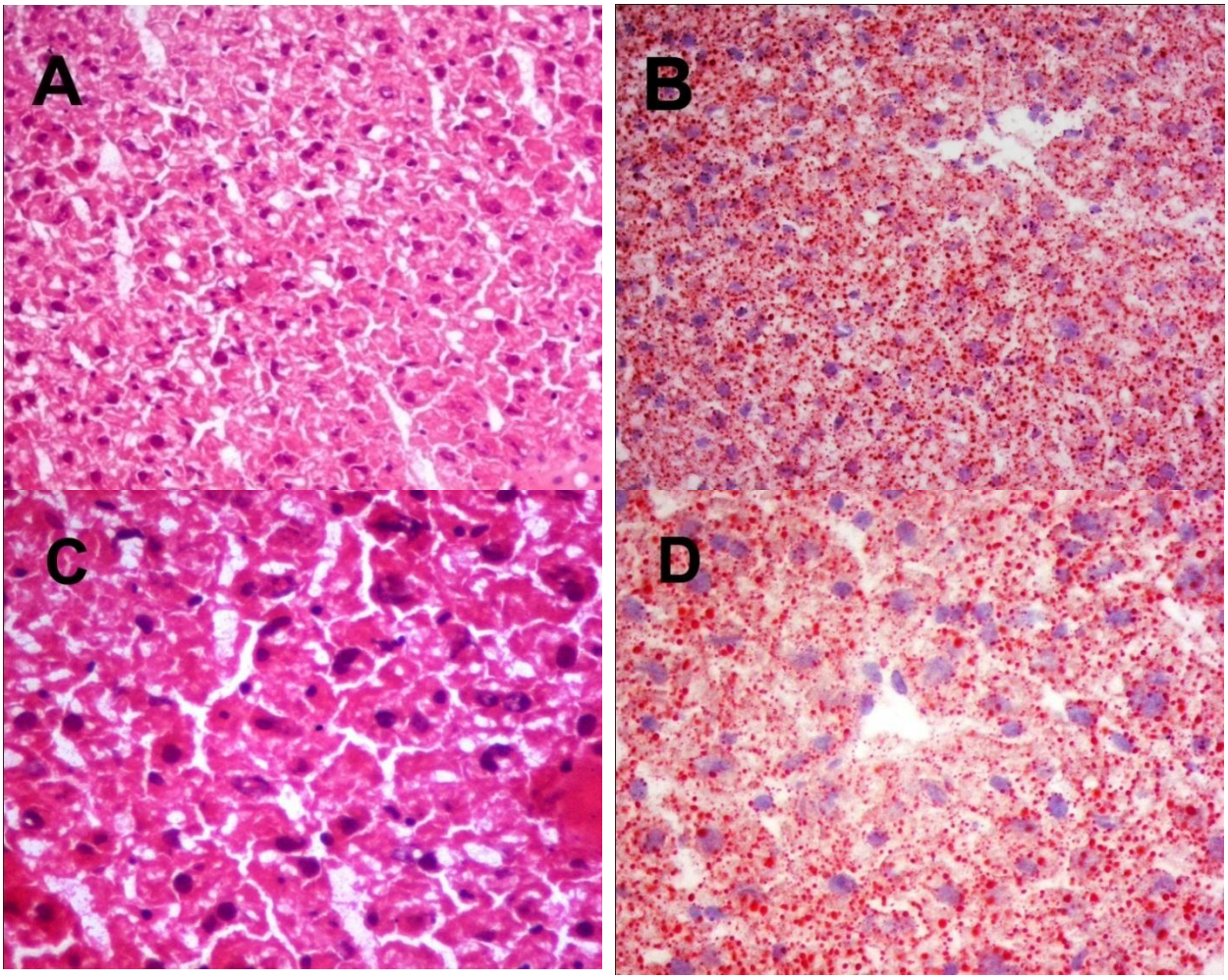

Figure S3: Histological analysis of liver from control group with normal diet. A: Hematoxylin and Eosin stain (X100) shows normal liver architecture. Some hepatocytes show microvesicular steatosis seen as minute clear unstained spaces. B: Oil Red O stain (X100), performed on frozen liver sections shows small red-stained fat droplets within hepatocytes as red-stained dots. C&D: higher magnification of the previous two photomicrographs respectively (X200).

© 2021 ACG Publications. All rights reserved.

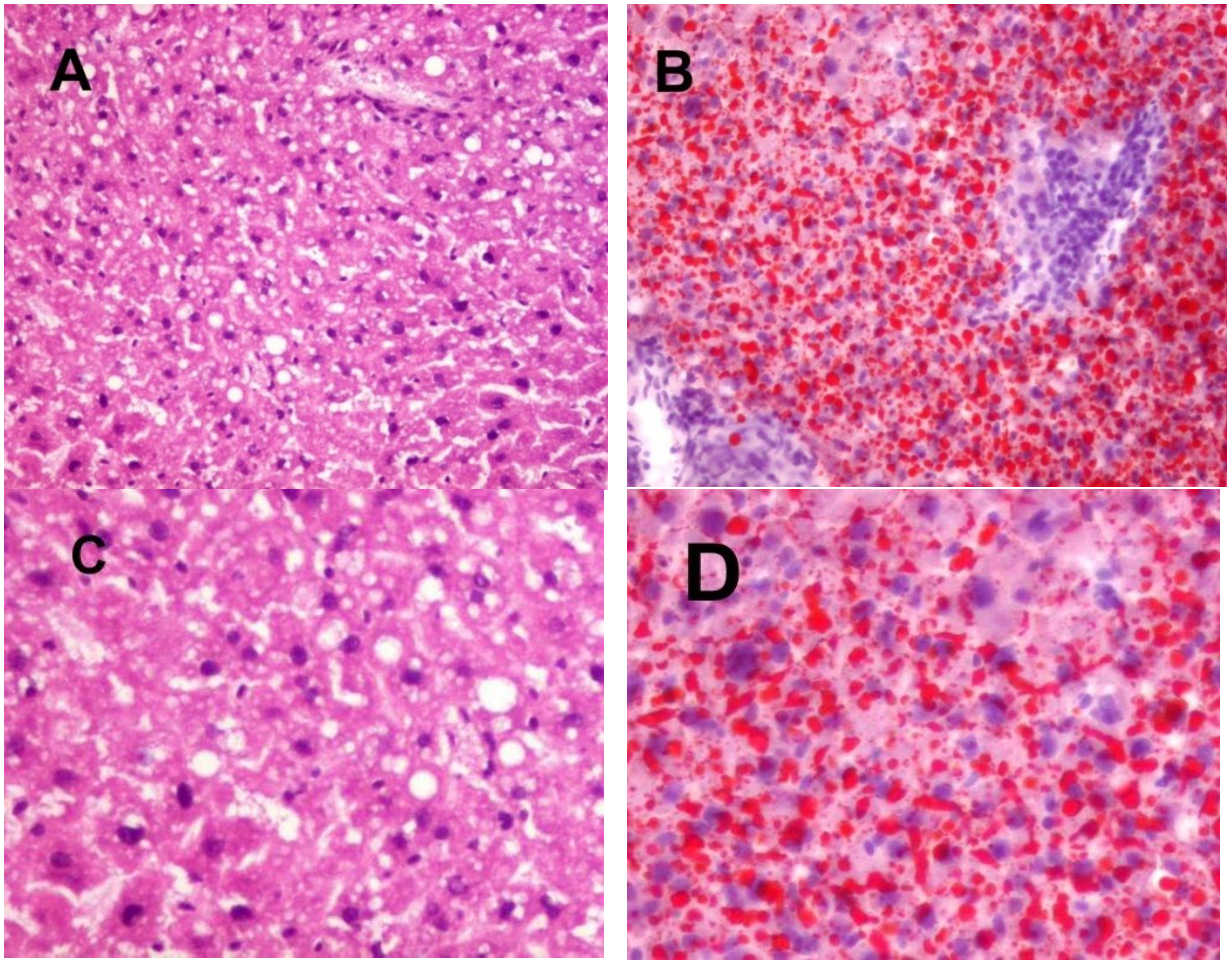

Figure S4: Histological analysis of liver from treated with green tea total extract group with HFD. A: Hematoxylin and Eosin stain (X100) shows near-normal liver architecture with small clear unstained fat vacuoles as compared to HFD group. B: Oil Red O stain (X100), performed on frozen liver sections shows fewer and small red-stained fat droplets within hepatocytes compared to HFD group. C&D: higher magnification of the previous two photomicrographs respectively (X200).

© 2021 ACG Publications. All rights reserved.

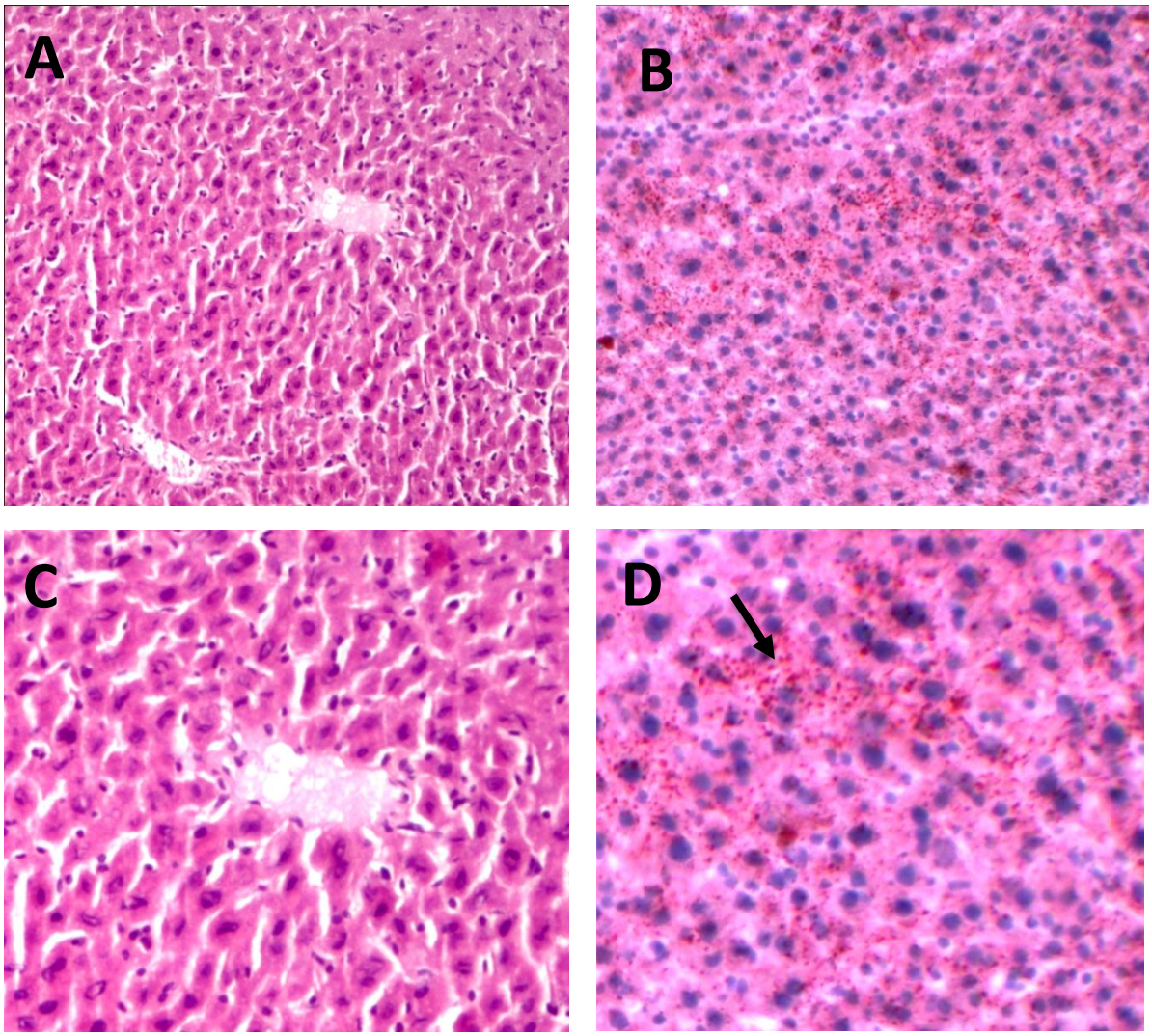

Figure S5: Histological analysis of liver from group treated with *M. cavendishii* total extract. A: Hematoxylin and Eosin stain (X100) shows near-normal liver architecture with no fat vacuoles as compared to HFD group. B: Oil Red O stain (X100), performed on frozen liver sections shows fewer and small red-stained fat droplets within hepatocytes compared to HFD group. C&D: Higher magnification of the previous two photomicrographs respectively (X200)

© 2021 ACG Publications. All rights reserved.

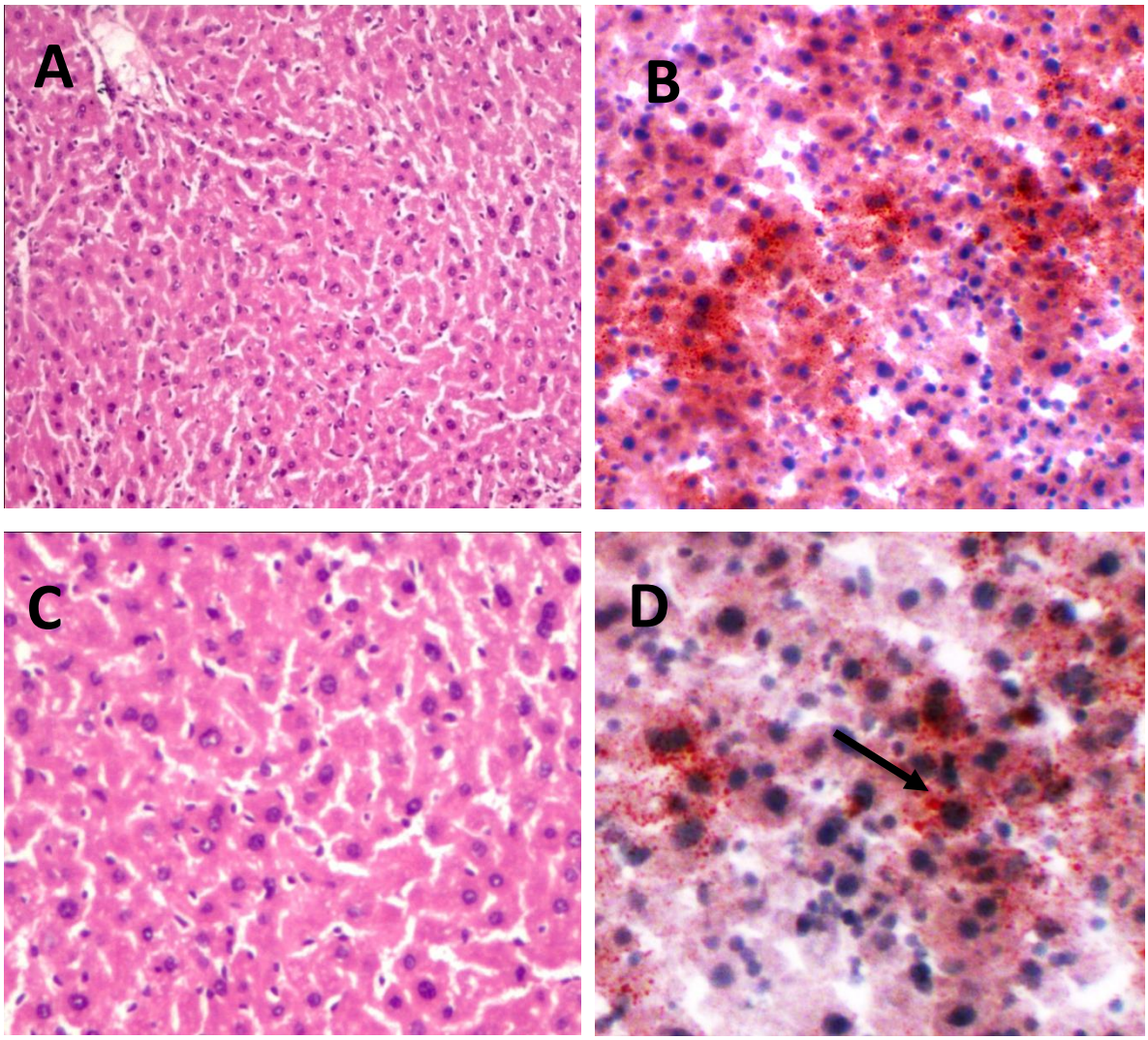

Figure S6: Histological analysis of liver from group treated with the ethyl acetate fraction of *M. cavendishii*. A: Hematoxylin and Eosin stain (X200) shows normal liver architecture. Few hepatocytes show minute clear unstained spaces. B: Oil Red O stain (X100), performed on frozen liver sections shows small red-stained fat droplets within hepatocytes as red-stained dots. C&D: higher magnification of the previous two photomicrographs respectively (X200).

© 2021 ACG Publications. All rights reserved.

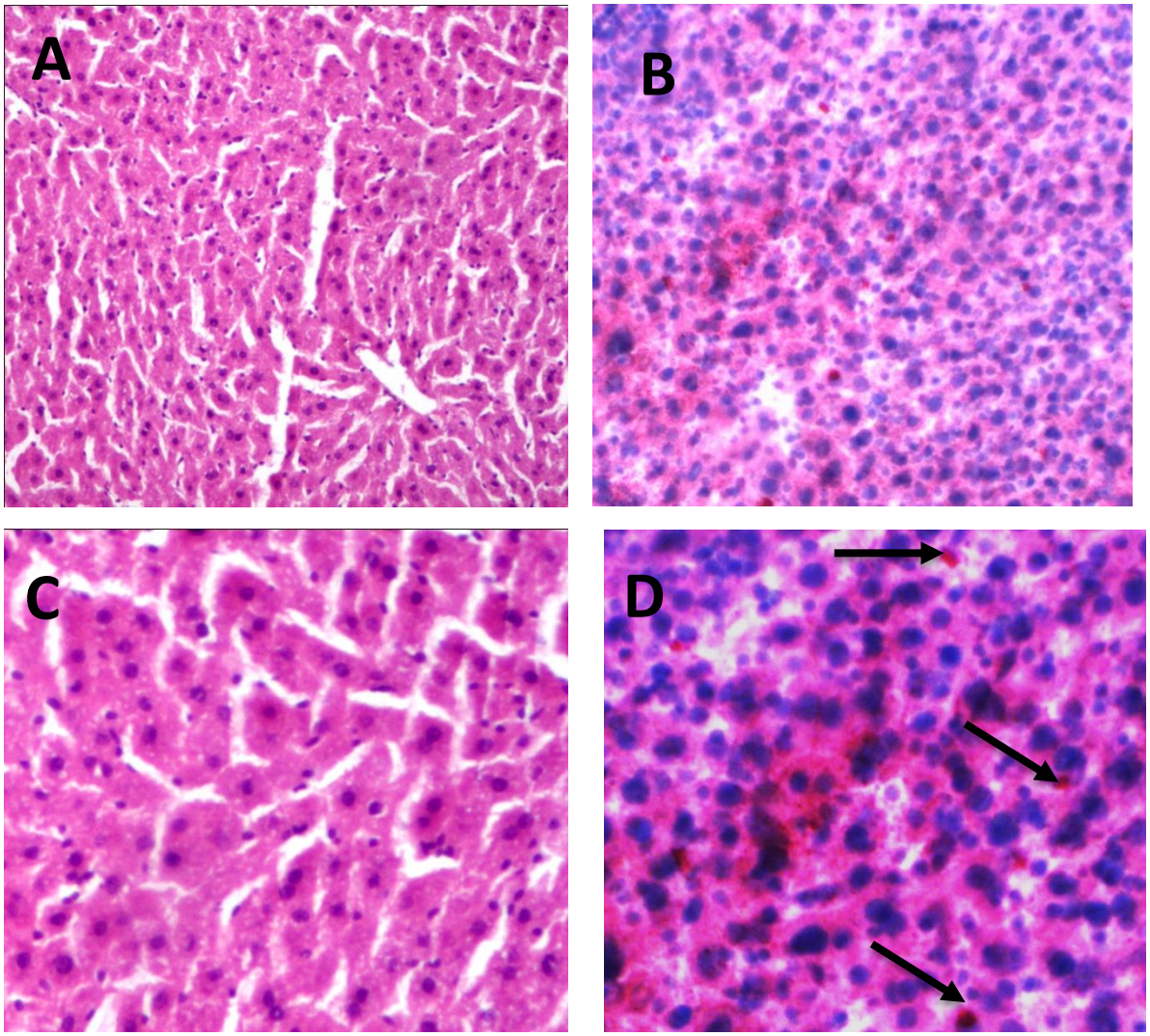

Figure S7: Histological analysis of liver from group treated with *n*-hexane fraction of *M. cavendishii*. A: Hematoxylin and Eosin stain (X100) shows near-normal liver architecture with small clear unstained fat vacuoles as compared to HFD group. B: Oil Red O stain (X100), performed on frozen liver sections shows few and small red-stained fat droplets within hepatocytes compared to HFD group. C&D: higher magnification of the previous two photomicrographs respectively (X200).

© 2021 ACG Publications. All rights reserved.

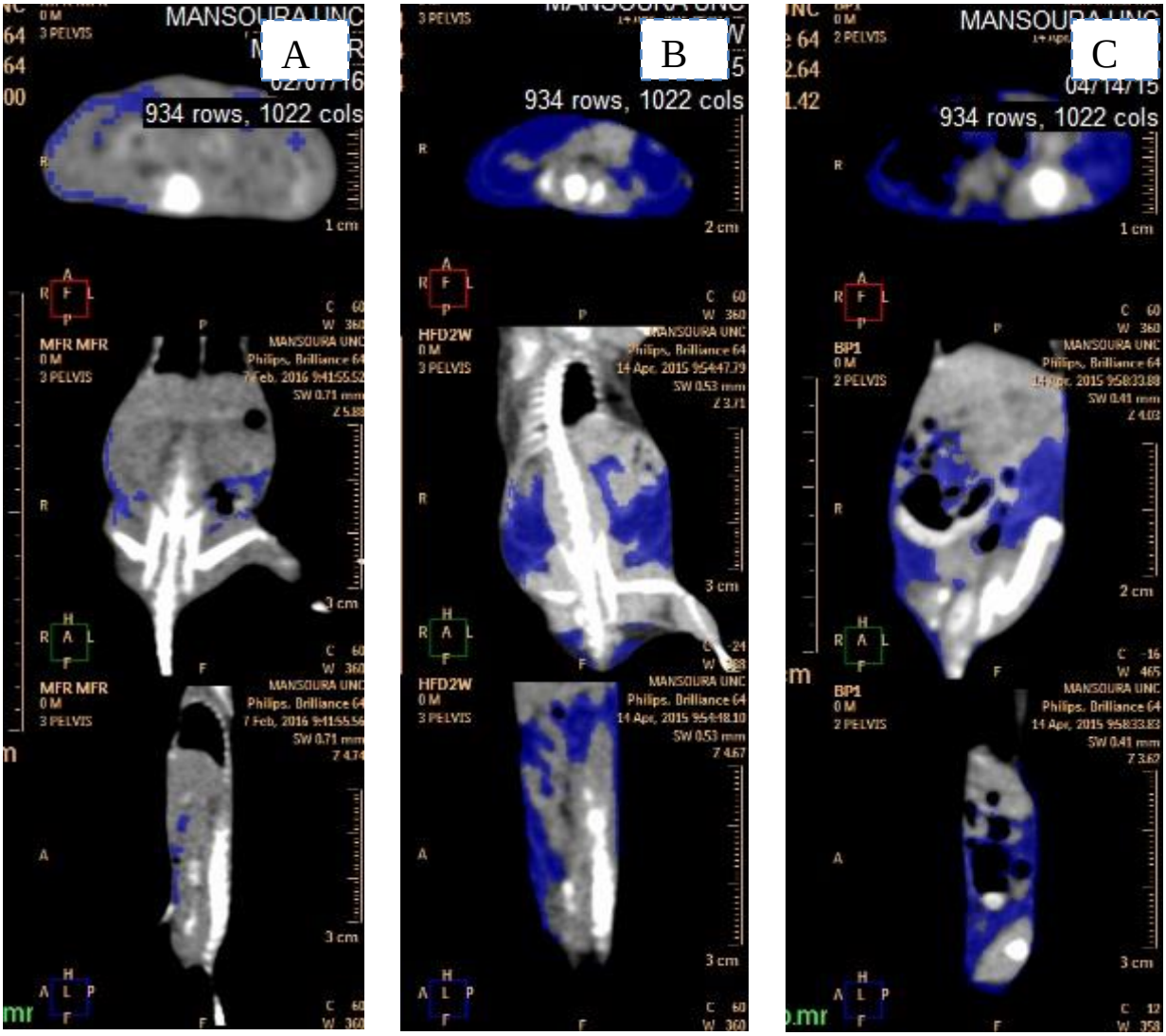

Figure S8: Representative CT images segmented for fat (axial, coronal and sagittal slices). A: *M. cavendishii* group CT, fat volume in blue, B: HFD CT, fat volume in blue, and C: LFD CT group, fat volume in blue.

© 2021 ACG Publications. All rights reserved.

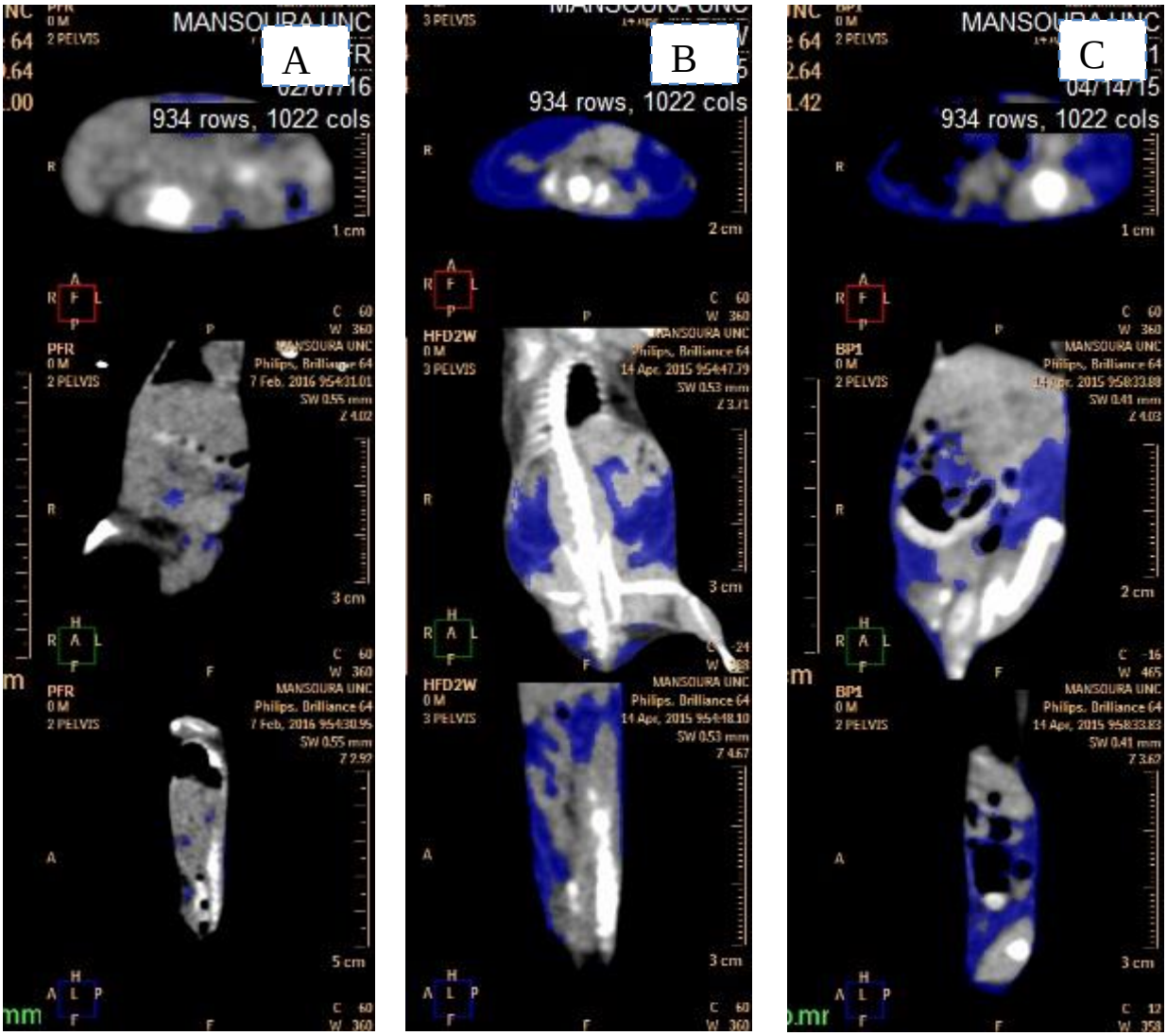

Figure S9: Representative CT images segmented for fat (axial, coronal and sagittal slices). A: *n*-hexane fraction of *M. cavendishii* group CT, fat volume in blue. B: HFD CT, fat volume in blue, and C: LFD CT group, fat volume in blue.

© 2021 ACG Publications. All rights reserved.

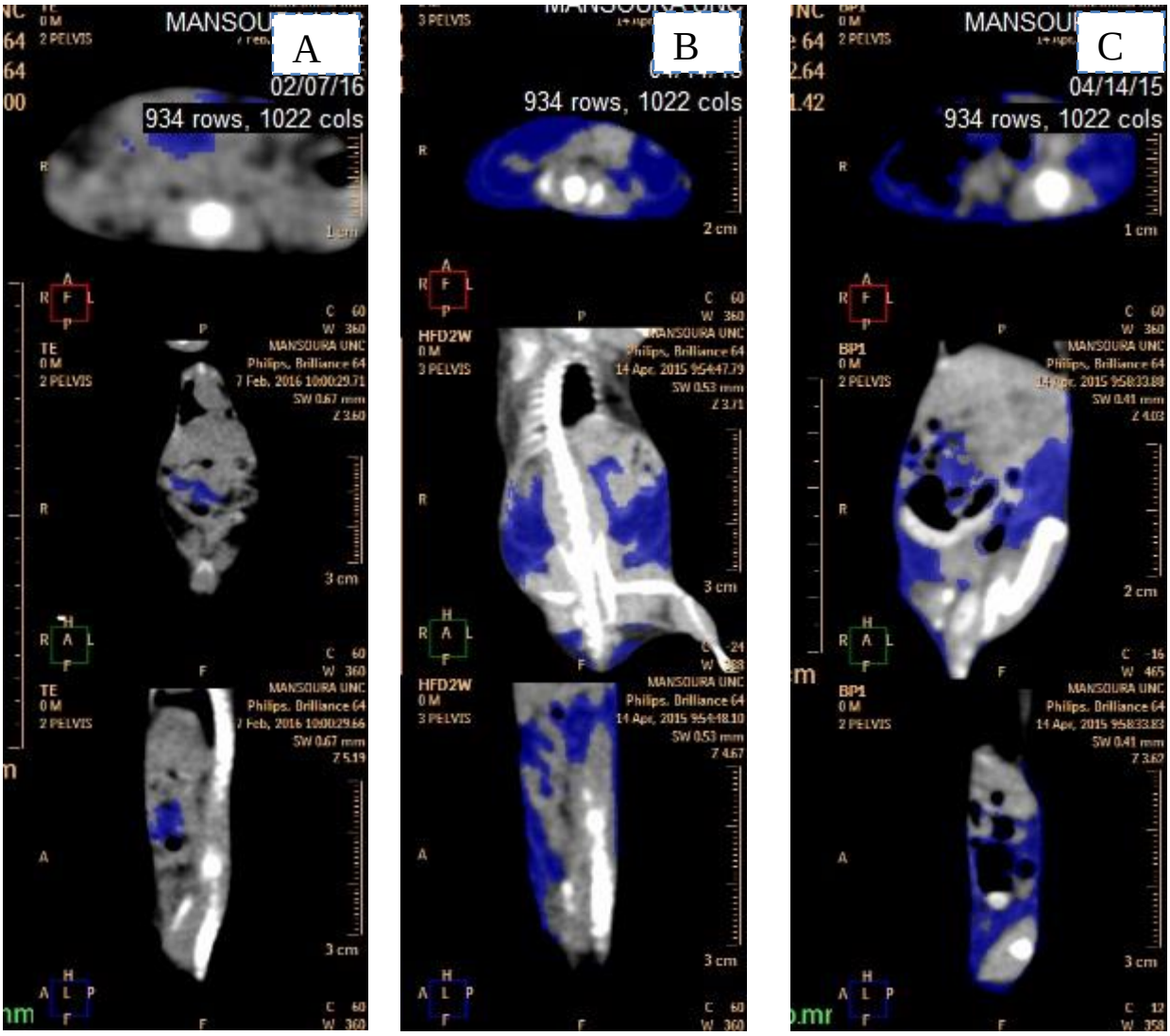

Figure S10: Representative CT images segmented for fat (axial, coronal and sagittal slices). A: Ethyl acetate fraction of *M. cavendishii* group CT, fat volume in blue, B: HFD CT, fat volume in blue and C: LFD CT group, fat volume in blue.

© 2021 ACG Publications. All rights reserved.

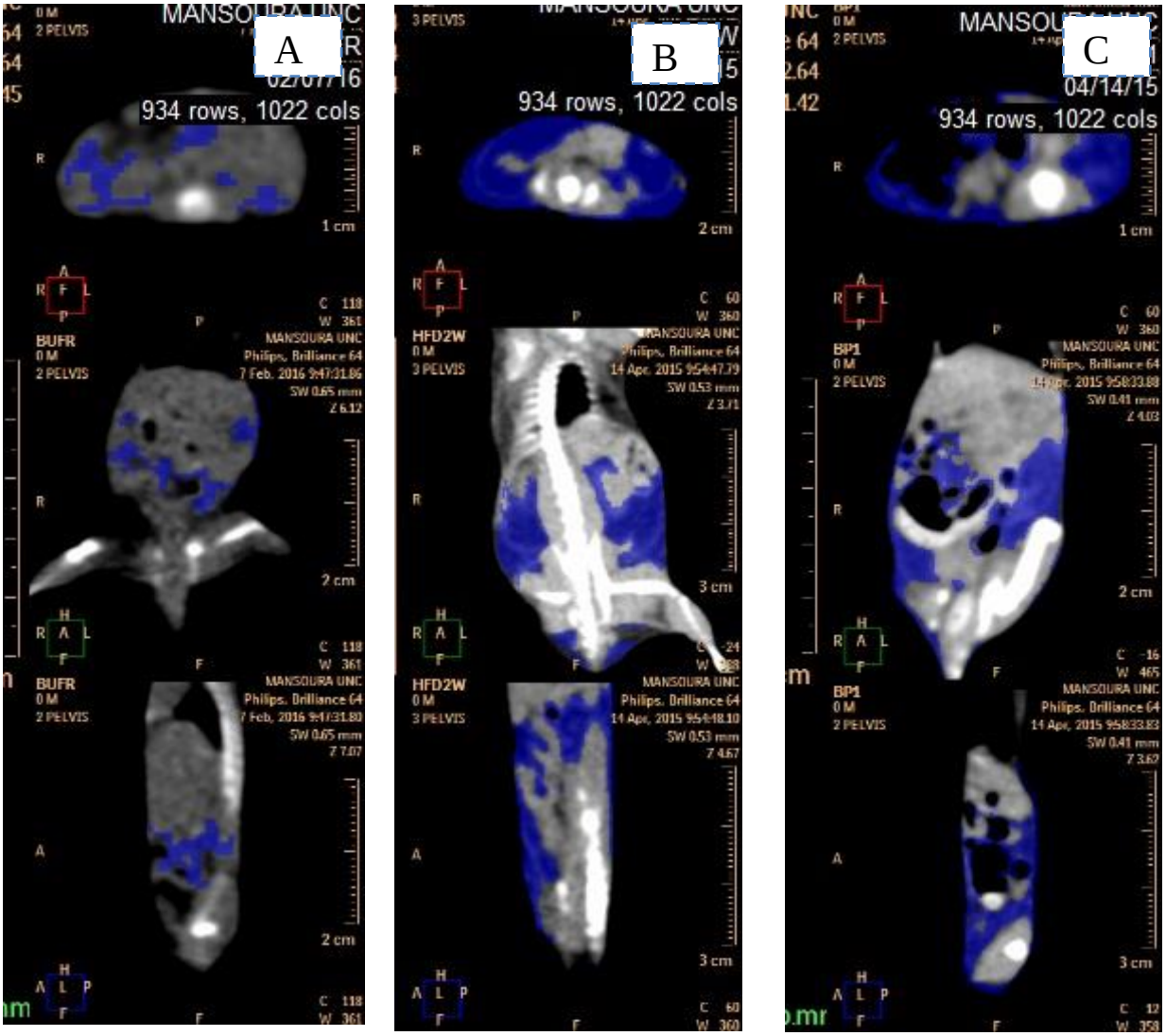

Figure S11: Representative CT images segmented for fat (axial, coronal and sagittal slices). A: Green tea total extract group CT, fat volume in blue, B: HFD CT, fat volume in blue and C: LFD CT group, fat volume in blue.

© 2021 ACG Publications. All rights reserved.

Phytochemical investigation of the *n*-hexane fraction of *Musa cavendeshii*

The *n*-hexane extract (Hex) of *M. cavendishii* (20 g) was fractionated over silica gel column (50 x 4.5 cm i.d., 300 g silica), using petroleum ether and eluted with *n*-hexane-EtOAc mixtures with increased polarity. Hundred mL fractions were collected and monitored by silica gel TLC [EtOAc-*n*-hexane, 1:9 v/v] or RP-18 TLC plates [MeOH-H_2O, 8.5: 1.5 v/v] and vanillin/sulfuric acid spray reagent. Similar fractions were pooled together, concentrated and subjected to further chromatographic fractionation.

Group 1 (54-62), 720 mg, eluted by 5% EtOAc, was re-chromatographed on RP-18 silica gel column (2.5 cm i.d. x 25 cm, 30 g) using water-methanol mixtures. Fractions, 10 mL, were analyzed RP-18 TLC [MeOH-H_2O, 8.5: 1.5 v/v]. Fractions 55-64, afforded compound **1** (12 mg, brown spot, R_f 0.85). Fractions 73-81, 68 mg, were re-chromatographed on medium pressure diol functionalized silica gel column (2.5 cm i.d. x 30 cm, 10 g, 3 mL/min). Elution was started with 100% *n*-hexane, 3 mL fractions were collected. Sub-fractions 50-80 eluted with *n*-hexane-EtOAc (99.5:0.5 v/v) contained compound **2** (3 mg, dark red, R_f 0.5) using RP-18 TLC, MeOH-H_2O (8.5: 1.5 v/v). Fractions 128-143, 80 mg, were chromatographed on medium pressure diol functionalized silica gel (2.5 cm i.d. x 30 cm, 10 g, and 3 mL/ min). Elution was started with 100% *n*-hexane, 3 mL fractions were collected. Sub-fractions 50-73 eluted with *n*-hexane-EtOAc (99:1 v/v) were pooled together to give compound **3** (7 mg, violet to brown, R_f 0.25) using RP-18 TLC, MeOH-H_2O (8.5: 1.5 v/v).

Group 2 (70-77), 70 mg, eluted by 5% EtOAc, showed one major spots (R_f 0.20) using silica gel TLC and *n*-hexane-EtOAc (95:5 v/v). It was purified by crystallization from CH_2Cl_2-MeOH mixture to give compound **4** (55 mg, violet, R_f 0.30) using *n*-hexane-EtOAc (9:1 v/v).

© 2021 ACG Publications. All rights reserved.

Table S1: ^{1}H NMR (500 MHz) and APT (125 MHz) spectral data of compound **2** in chloroform-*d*

C/H #	APT	^{1}HNMR
1	29.3, CH_2	2.56, m
2	33.1, CH_2	HA: 1.96 HB: 2.04
3	87.1, qC	---
4	41.1, CH_2	1.60, m
5	21.5, CH_2	1.27, m
6	37.3, CH_2	1.25, m
7	32.9, CH	1.40, m
8	37.7, CH_2	1.19, m
9	24.9, CH_2	1.27, m
10	37.5, CH_2	1.03, m
11	32.8, CH	1.40, m
12	37.4, CH_2	1.25,m
13	24.6, CH_2	1.15, m
14	39.5, CH_2	1.10, m
15	28.1, CH	1.48, m
16	22.8, CH_3	0.85, d(6.5)
17	22.7, CH_3	0.85, d (6.5)
18	19.8, CH_3	0.82, d (6.5)
19	19.7, CH_3	0.82, d (6.5)
20	25.7, CH_3	1.37, s
21	177.0, qC	---

© 2021 ACG Publications. All rights reserved.

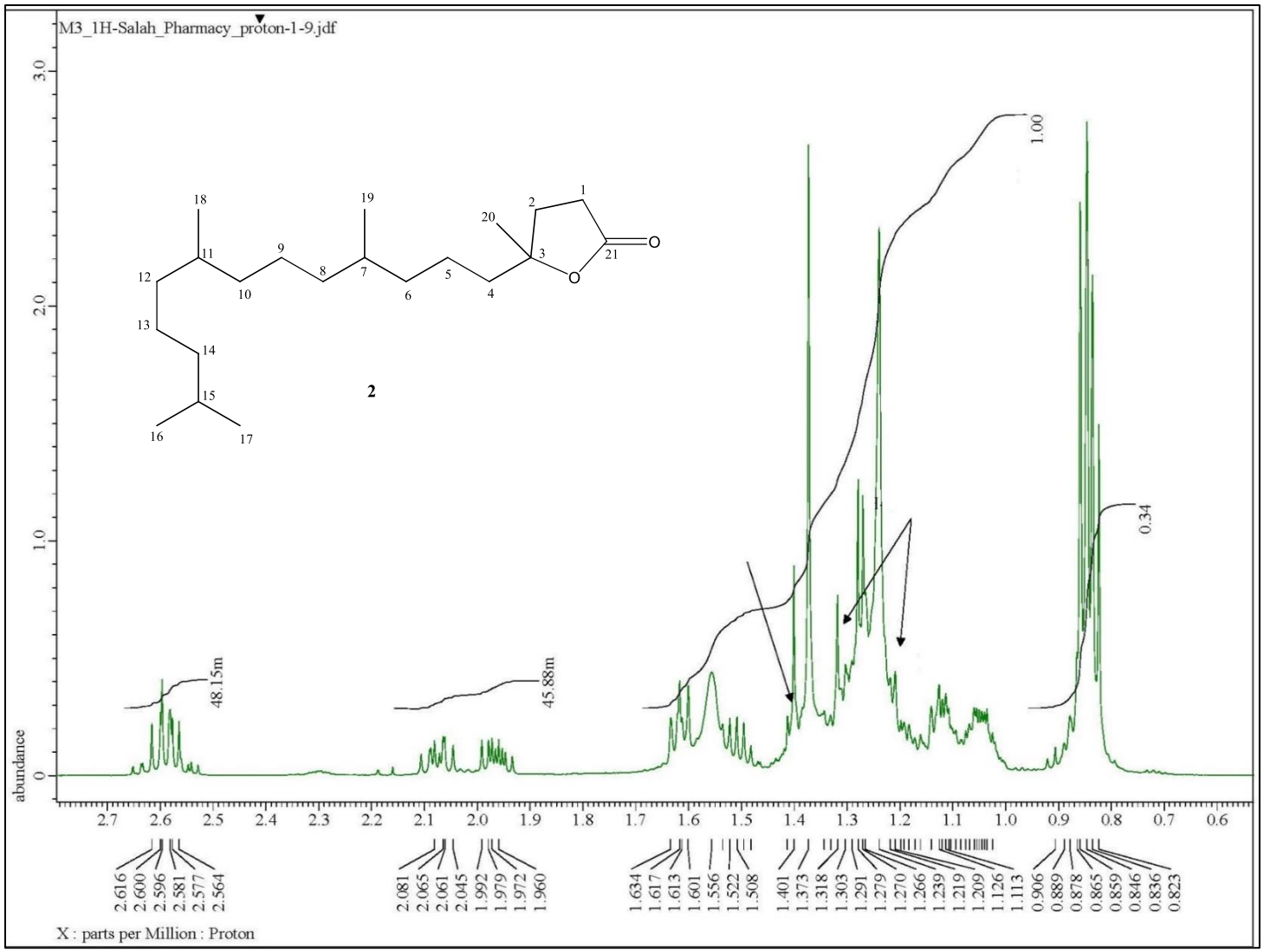

Figure S12: ^{1}H NMR (500 MHz) spectrum of compound **2** in $CDCl_3$.

© 2021 ACG Publications. All rights reserved.

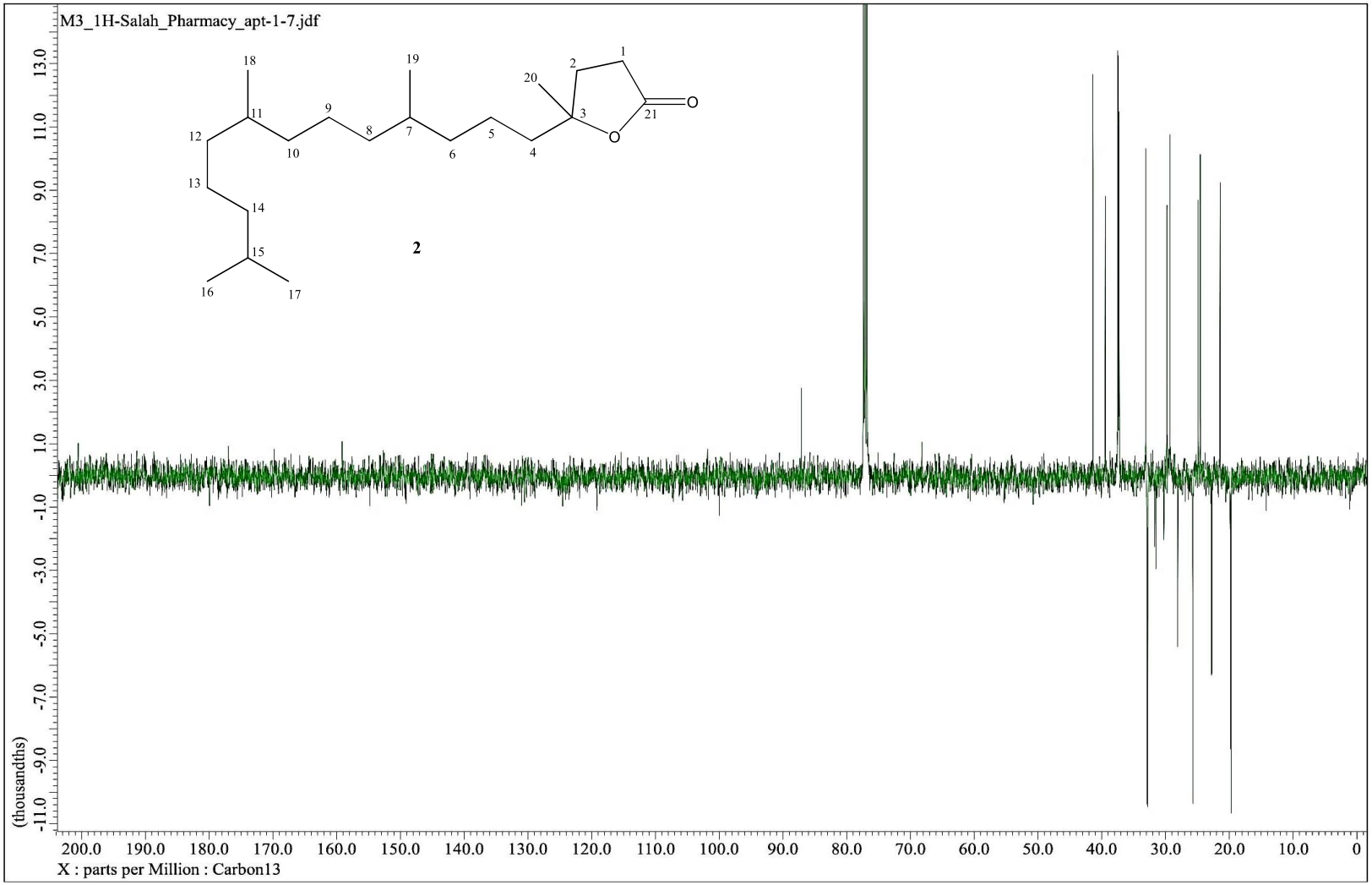

Figure S13: APT (125 MHz) spectrum of compound **2** in $CDCl_3$.

© 2021 ACG Publications. All rights reserved.

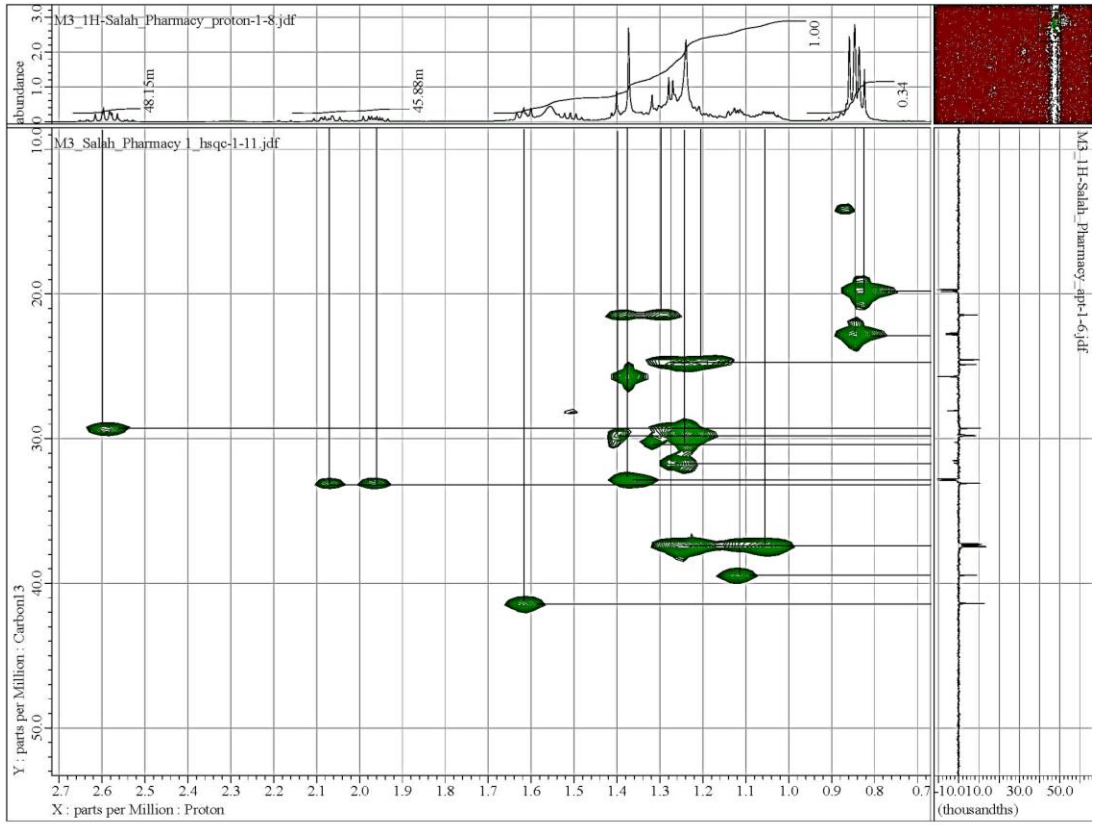

Figure S14: HSQC spectrum of compound **2**.

© 2021 ACG Publications. All rights reserved.

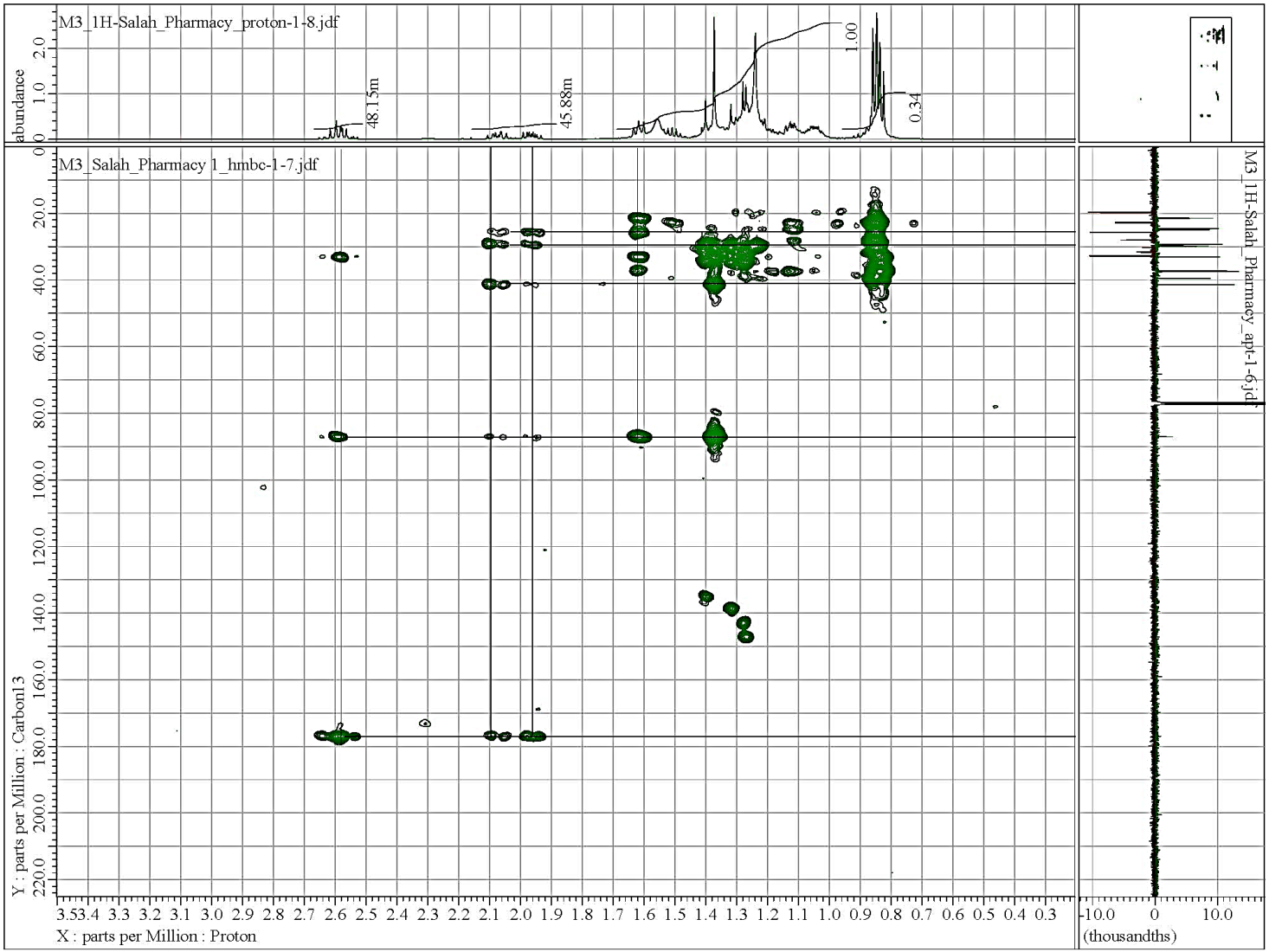

Figure S15: HMBC spectrum of compound **2** in $CDCl_3$.

© 2021 ACG Publications. All rights reserved.

Analysis Info

Analysis Name	D:\Data\Williams\2-M3-POS.d	Acquisition Date	8/2/2017 11:34:57 AM
Method	tune_wide_pos_Jan2017.m	Operator	BDAL@DE
Sample Name		Instrument	micrOTOF-Q 228888.00070
Comment			

Acquisition Parameter

Source Type	ESI	Ion Polarity	Positive	Set Nebulizer	2.0 Bar
Focus	Not active	Set Capillary	4500 V	Set Dry Heater	200 °C
Scan Begin	50 m/z	Set End Plate Offset	-500 V	Set Dry Gas	4.0 l/min
Scan End	3500 m/z	Set Collision Cell RF	550.0 Vpp	Set Divert Valve	Source

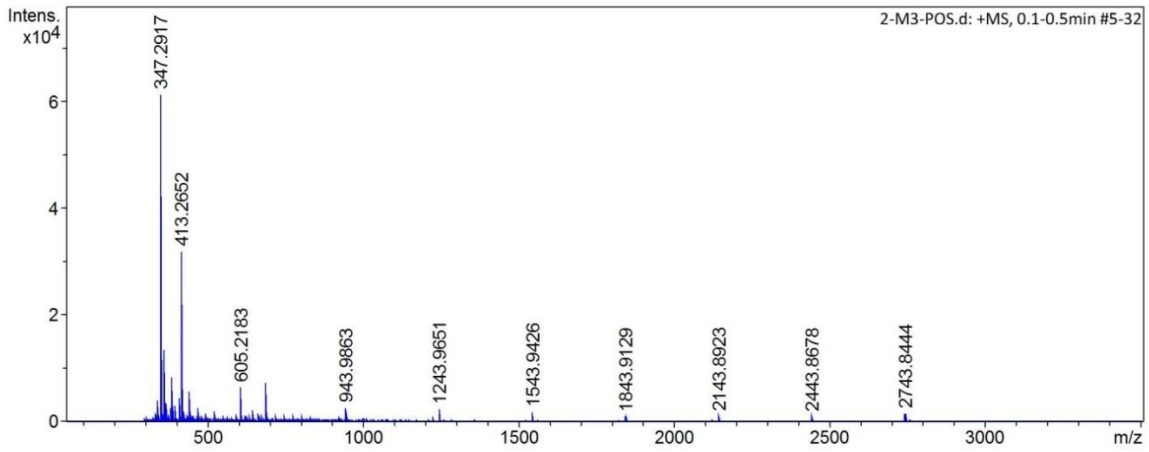

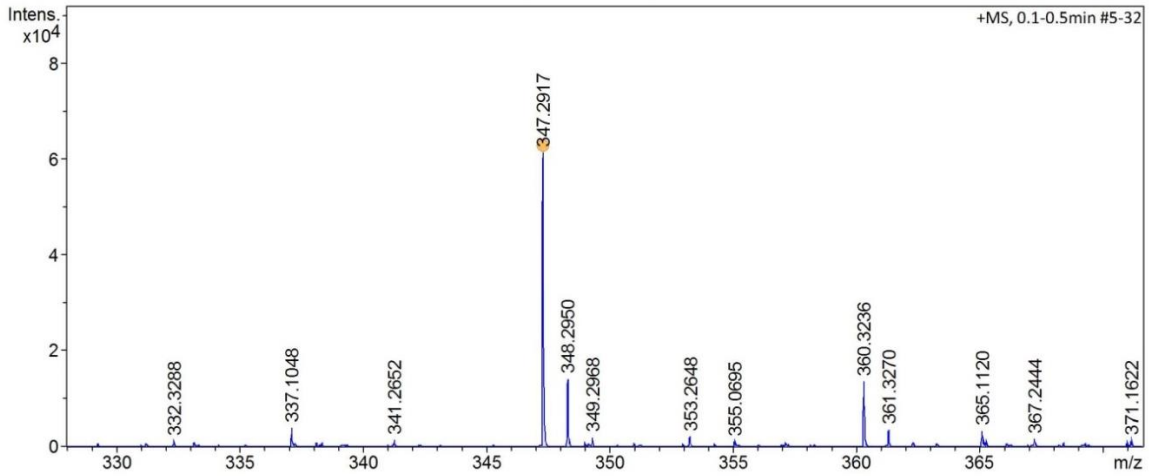

Meas. m/z	#	Ion Formula	m/z	err [ppm]	mSigma	# mSigma	Score	rdb	e¯ Conf	N-Rule
347.2917	1	C19H35N6	347.2918	0.2	4.0	1	100.00	5.5	even	ok
	2	C21H37N3O	347.2931	4.0	7.9	2	46.15	5.0	odd	ok
	3	C18H39N2O4	347.2904	-3.7	12.3	3	46.11	0.5	even	ok
	1	C19H35N6	347.2918	0.2	4.0	1	100.00	5.5	even	ok
	2	C21H37N3O	347.2931	4.0	7.9	2	46.15	5.0	odd	ok
	3	C18H39N2O4	347.2904	-3.7	12.3	3	46.11	0.5	even	ok

Figure S16: HRMS spectrum of compound **2**.

© 2021 ACG Publications. All rights reserved.

Table S2: ^{1}H NMR (500 MHz) and APT (125 MHz) spectral data of compound **3** in chloroform-*d*

position	Multiplicity (APT)	δ_H		δ_C	
		M_4	**Cycloeucalenol (Hoa, et al., 2014)**	**M_4**	**Cycloeucalenol (Hoa, et al., 2014)**
C-1	CH_2			30.9	30.8
C-2	CH_2			34.9	34.8
C-3	CH	3.19, ddd, (13.5, 9, 4.5)	Not provided	76.7	76.6
C-4	CH			44.7	44.6
C-5	CH			43.4	43.4
C-6	CH_2			24.8	24.7
C-7	CH_2			27.4	28.1
C-8	CH			47.0	46.9
C-9	C	---	---	23.6	23.6
C-10	C	---		29.6	29.7
C-11	CH_2			25.3	25.2
C-12	CH_2			32.9	32.9
C-13	C	---	---	45.2	45.4
C-14	C	---	---	49.0	48.9
C-15	CH_2			35.4	35.0
C-16	CH_2			27.0	27.2
C-17	CH			52.3	52.2
C-18	CH_3	0.96, 3H, s	0.97, 3H, s	17.9	17.8
C-19	CH_2	H_A-19: 0.13, d (4.0) H_B-19: 0.37, d (3.5)	H_A-19: 0.14, d (4.0) H_B-19: 0.39, d (4.0)	28.2	27.0
C-20	CH			36.2	36.1
C-21	CH_3	0.88, 3H, d (4.5)	0.91, 3H, d (4.5)	18.4	18.4
C-22	CH_2			35.1	35.4
C-23	CH_2			31.4	31.3
C-24	C	---	---	157.0	156.9
C-24a	CH_2	H_A-24a: 4.65, brs H_B-24a: 4.70, brs	H_A-30: 4.67, s H_B-30: 4.72, s	106.0	105.9
C-25	CH	2.20, 1H, septet	Not provided	33.9	33.8
C-26	CH_3	1.02, 3H, d (6.5)	1.03, 3H, d (7.0)	22.1	22.0
C-27	CH_3	1.00, 3H, d (6.5)	1.02, 3H, d (7.0)	22.0	21.9
C-28	CH_3	0.88, 3H, s	0.78, 3H, s	19.2	19.1
C-29	CH_3	0.97, 3H, d (7.0)	0.98, 3H, d (7.5)	14.5	14.4

© 2021 ACG Publications. All rights reserved.

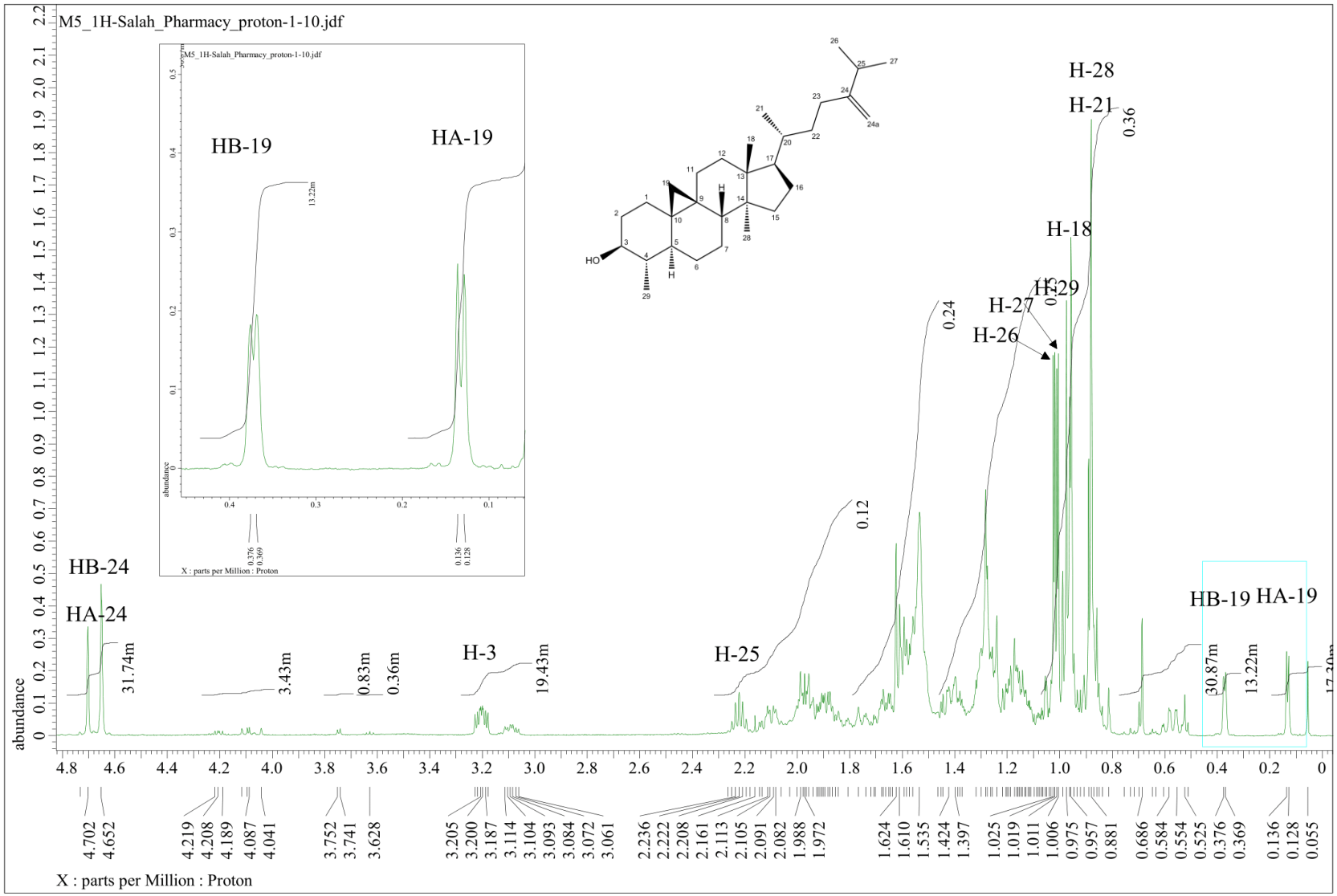

Figure S17: ^{1}H NMR (500 MHz) spectrum of compound **3** in $CDCl_3$.

© 2021 ACG Publications. All rights reserved.

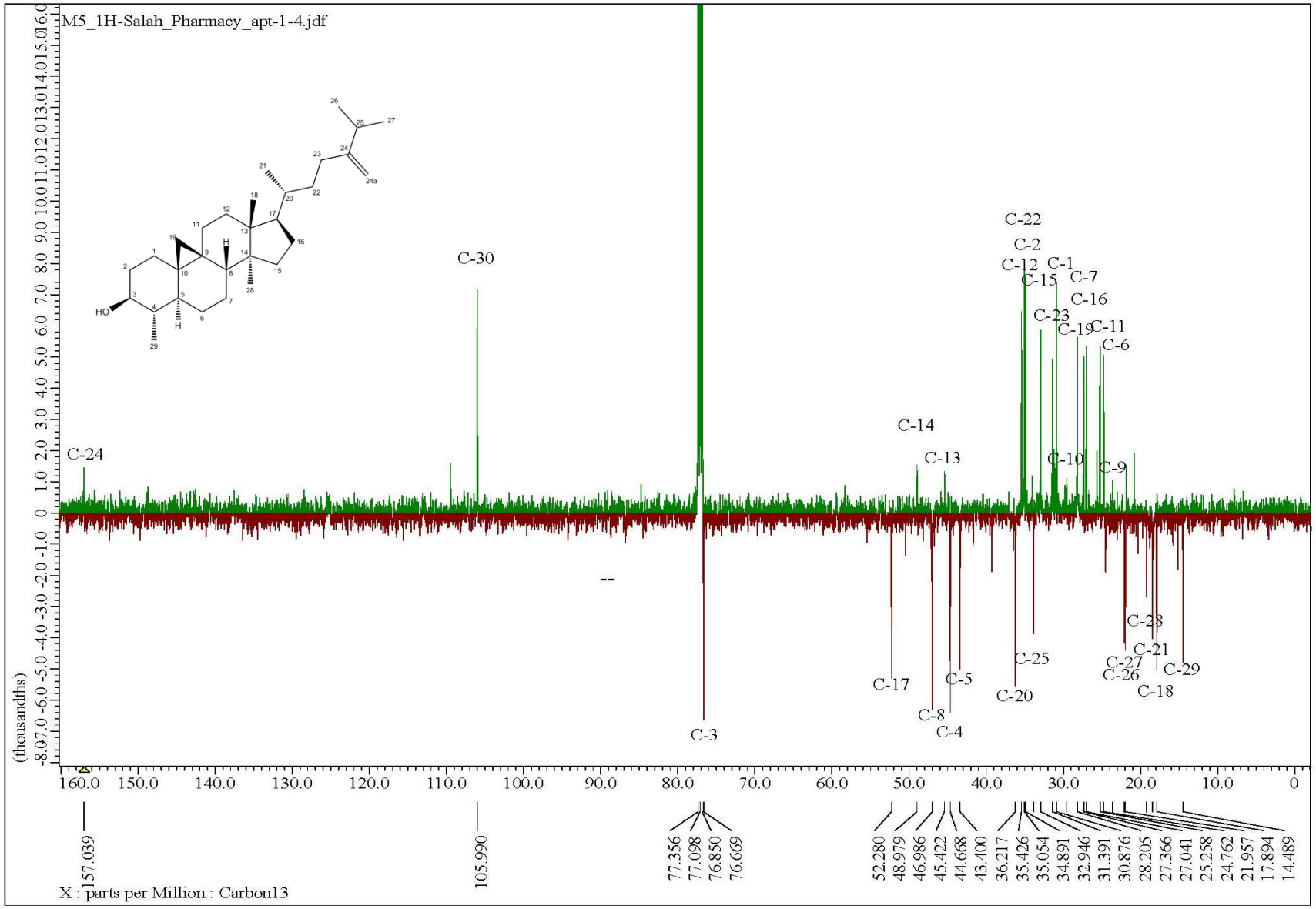

Figure S18: APT (125 MHz) spectrum of compound **3** in $CDCl_3$.

© 2021 ACG Publications. All rights reserved.